

Discrimination between Inhibitory and Excitatory Neurons of Mouse Hippocampus Based on the Shape of Extracellular Spike Waveforms

Mehrdad Oghazian, Farzad Saffari, Ali Khadem * 

Department of Biomedical Engineering, Faculty of Electrical Engineering, K. N. Toosi University of Technology, Tehran, Iran

*Corresponding Author: Ali Khadem
Email: alikhadem@kntu.ac.ir

Received: 29 January 2021 / Accepted: 19 April 2021

Abstract

Purpose: Inhibitory and excitatory neurons play an essential role in brain function, and we aim to introduce an automatic method to discriminate these two populations based on features of the shape of their spikes. Consequently, we will explain the spike extraction from raw data of a single shank electrode and determine the best features of spike waveforms for the classification of neurons. It is noteworthy that, to the best of our knowledge, classification of inhibitory and excitatory neurons using the shape features extracted from their spike waveforms has not been done before.

Materials and Methods: In this paper, we use a dataset of mouse hippocampus neurons in which the neuron types (inhibitory or excitatory) have been verified optogenetically. For the classification of mouse hippocampus neurons, we extracted eight shape features of their spike waveforms in addition to their firing rates and used three types of classifiers: K-Nearest Neighbors (KNN), Linear Discriminant Analysis (LDA), and Support Vector Machine (SVM) to analyze the discriminatory power of features based on the accuracy of the classifications.

Results: We showed that Spike asymmetry, Peak-to-trough ratio, Recovery slope, and Duration between peaks were four shape features of spike waveforms participated in the optimum feature subsets that resulted in maximum classification accuracy. Moreover, the SVM classifier with RBF kernel resulted in maximum accuracy of $96.91 \pm 13.03\%$ and was identified as the best classifier.

Conclusion: In this study, we found that shape features of spike waveforms can accurately classify inhibitory and excitatory neurons of mouse hippocampus. Also, we found an optimum subset of shape features of spike waveforms that resulted in better classification performance than previously proposed subsets of features used for clustering of neurons. Our findings open a promising way toward a functional classification of neurons automatically.

Keywords: Inhibitory and Excitatory Neurons; Classification; Mouse Hippocampus; Shape Features; Spike Waveform; Extracellular Recordings.

1. Introduction

It is impossible to know the brain without knowing its components, especially the neurons that play the most important role in the brain. By studying the behavior of a healthy brain, the normal behavior of neurons can be understood which consequently helps to detect abnormal cases. Inhibitory and excitatory neurons are the two main groups of neurons that show different functions during brain activity due to inherent differences in their behavior. The activity of inhibitory neurons reduces the firing rate of postsynaptic neurons while the activity of excitatory neurons increases the firing rate of postsynaptic neurons [1]. In this research, we study the behavior of inhibitory and excitatory neurons from the perspective of electrophysiological properties to identify the differences in the shape of their spike waveforms. Features obtained from the shape of spike waveforms, average firing rate, firing rate changes, etc. are in the category of electrophysiological properties of neurons. In this study, we intend to use the shape of the spike waveform of each neuron to determine its type (inhibitory or excitatory) with the help of an appropriate classification scheme.

Various shape features of the spike waveform of neurons have been used in the literature to separate inhibitory and excitatory neurons, but the classification accuracy of their subsets has not been evaluated by an accurate validation method yet. In this study, we intend to compare shape features of the spike waveform of neurons with each other to determine the best ones for discriminating inhibitory and excitatory neurons from each other. For this purpose, we are going to introduce and extract appropriate shape features from the spike waveform of neurons that result in high classification accuracy by using the most common classifiers. Moreover, we will search for the most suitable classifier that can accurately separate excitatory and inhibitory neurons.

In this research, in addition to previously defined shape features of spike waveforms, we also intend to provide some new shape features for functional separation (inhibitory and excitatory) of neurons and to evaluate and compare the discriminative power of the relevant features on the dataset recorded from the rat brain hippocampus, which has true inhibitory and excitatory labels. As far as we know, such an approach (classification of neurons using shape features of spike waveforms) has not been done in the previous studies.

In the following parts of this paper, first, we introduce the properties of the mouse brain data. Afterward, the relevant shape features in use for the classification will be described briefly. Then, we will introduce some classifiers and evaluate their performance regarding every single feature and their subsets for the inhibitory/excitatory classification. Lastly, we will wrap up this article by providing a discussion on the optimum features and classifier selection, which could lead us to expand this research.

2. Materials and Methods

In this study, different shape features of the spike waveform of neurons and classifiers are examined for recognizing the excitatory or inhibitory neurons. We categorize neurons into inhibitory (class 1) and excitatory (class 2) within five steps: extracting shape features of spike waveforms, selecting subsets of features, balancing the data, classification, and validation. Nine features (F1 to F9) were extracted from the spikes of mouse hippocampus neurons (650 excitatory and 26 inhibitory, verified optogenetically) to be used as inputs of the KNN, LDA, and SVM (linear and RBF) classifiers [2]. We divided 650 excitatory neurons into 25 groups of 26 neurons each and repeated the classification procedure for each group of 26 excitatory neurons and 26 available inhibitory neurons in order to have 25 balanced classifications. Since in each classification, we had just 52 data samples to train and validate each classifier, we used LOOCV (leave-one-out cross-validation) for efficient validation of classifications. Furthermore, we repeated LOOCV for all 25 (650/26) parts of excitatory neurons, and finally, all 25 obtained average accuracies of each classifier were averaged.

2.1. Mouse Brain Data

This data was recorded from the hippocampus of mice in the PV: ChR2 line at the age of 6-12 months by a 32-channel silicon electrode integrated with light-emitting diodes or a 64-channel silicon electrode paired with optical fibers while the mice moved freely. At the data collection stage, the extracellular signals were prepared by the IR-183 amplifier, band-pass filtered in the frequency range of 0.01–6 kHz, and recorded after sampling by an Intan RHD2000 device [3]. Spike sorting algorithms have been used to detect spike waveforms by clustering and then assigning all the waveforms of one cluster to an individual neuron. Spike clustering was performed by Kilosort

software [4] from broadband data (sampling frequency 20-30 kHz) recorded from CA1 (first region of the hippocampus) of the rat's brain. In mouse data, which contains 676 spike waveforms of neurons, the type of neurons was determined by optogenetics (26 inhibitory neurons and 650 excitatory neurons) [3]. The data was recorded at Buzaki lab at NYU neuroscience institute, and all animal handling procedures were approved by the Institutional Animal Care and Use Committee of New York University Medical Center.

2.2. Feature Extraction

The first step in the classification problem is feature extraction. Feature extraction is an essential step in determining classifier inputs. We proposed two new features, "one minus left peak of the spike waveform" and "time interval between left and right maxima", in addition to 7 already existing features for the classification of neurons into inhibitory and excitatory categories. Before giving the features as inputs to the classifiers, the significance of difference in the mean of each feature between the inhibitory and excitatory groups was tested using the Wilcoxon rank-sum test and all the features passed this test (p-value < 0.015). We aim to identify a subset of features that result in the best classification accuracy in separating inhibitory and excitatory neurons (listed in Table 1) and will describe them briefly hereunder.

Table 1. Nine features used for the classification: F1 to F9. The p-values obtained from the Wilcoxon rank-sum test are reported

Feature Number	Features	P-value
F1	Duration	3.82e-16
F2	Half-width duration	9.11e-19
F3	Peak amplitude asymmetry	6.77e-16
F4	Peak-to-trough ratio	2.40e-12
F5	Recovery slope	1.42e-2
F6	Repolarization slope	3.50e-15
F7	Duration between peaks	1.63e-15
F8	1 - (left peak)	7.63e-18
F9	Firing rate	8.83e-15

2.2.1. Duration

The duration of each waveform is defined as the time between the depression of the spike waveform and the peak after it (Figure 1).

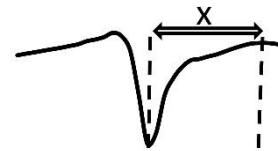


Figure 1. The duration of spike waveform [5]

2.2.2. Half-Width Duration

Half-width duration is the width of the spike waveform at half-maximum height (Figure 2) [6].

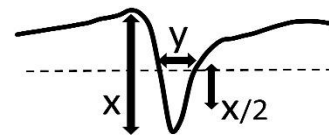


Figure 2. The Half-width duration of spike waveform [6]

2.2.3. Peak Amplitude Asymmetry

Peak amplitude asymmetry is defined as the ratio between the difference of the maxima and the sum of the maxima of the spike waveform (Figure 3).



Figure 3. The Peak amplitude asymmetry of the spike waveform [7]

2.2.4. Peak-to-Trough Ratio

The peak-to-trough ratio is defined as the ratio between the amplitude of the spike waveform at maximum to that at minimum (Figure 4).

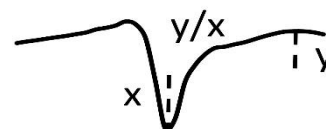


Figure 4. The Peak-to-trough ratio of spike waveform [8]

2.2.5. Recovery Slope

The recovery slope is equal to the tangential slope on the spike waveform between the maximum point and the subsequent turning point (Figure 5).

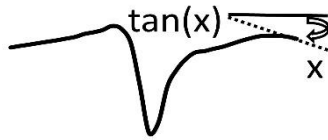


Figure 5. The Recovery slope of the spike waveform [8]

2.2.6. Repolarization Slope

The repolarization slope is the tangential slope on the spike curve between the bottom of the waveform and the subsequent turning point (Figure 6).

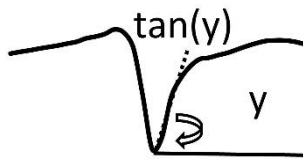


Figure 6. The Repolarization slope of the spike waveform [8]

2.2.7. Duration between Peaks

The duration between peaks is the time interval between the left and right maxima which is a new feature suggested by us (Figure 7).

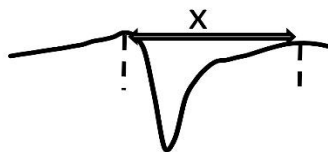


Figure 7. The Duration between peaks of the spike waveform

2.2.8. One Minus Left Peak

1-(left peak) is equal to one minus the left maximum value which is another new feature suggested by us (Figure 8).

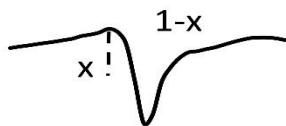


Figure 8. The feature one minus left peak of spike waveform

2.2.9. Firing Rate

The number of spikes per second is called the firing rate. The firing rate of a neuron is not constant over time and changes. The way that the firing rate changes varies between neurons. For example, in the bursting category, a large number of spikes are released in a few tens of

milliseconds and the neuron is silenced again. To derive the firing rate of each neuron during an experiment, we count the number of spikes and divide them by the time of the experiment. Although firing rate is not a shape feature of spike waveforms, we also evaluate its performance in our paper due to its importance.

2.3. Generating all Subsets of Features

In this paper, we try to find the best single features and also the best subset of features to discriminate excitatory and inhibitory neurons. Therefore, the next step after extracting the features is to generate a subset of them for giving as inputs to the classifiers. Generating a subset of features means selecting groups of features with m members ($1 \leq m \leq 9$). The total number of possible subsets is equal to $2^m - 1$. We divide features into subsets of 1 to 9 members. These features are used as input for classifiers. Among all possible feature subsets, we are looking for the subset which results in the highest classification accuracy.

2.4. Balancing the Data

The number of members of the inhibitory and excitatory groups is 26 and 650, respectively. If we train a classifier with all this dataset together, it will be biased toward assigning most test samples to the excitatory category. It means, in most cases, the type of neurons in the test data will be decided as excitatory by the classifier, and to avoid this, we balance the data between these categories. For this purpose, we divided the excitatory neurons into 25 groups of 26 members each and performed training and testing on 25 batches of 26 inhibitory and 26 excitatory neurons, and LOOCV was performed so that each time a different neuron was selected from a total of 52 neurons as test data so that all members could enter the test phase and the accuracy of LOO repetitions was averaged [9]. Finally, averaging was performed on the 25 average classification accuracies obtained by LOOCV.

2.5. Classifiers

In addition to linear classifiers such as LDA and linear Support Vector Machine (SVM), we also used nonlinear classifiers such as KNN and SVM with Radial Basis Function (RBF) kernel to classify non-linearly separable data. Hereunder, we will briefly introduce the applied classifiers.

2.5.1. Linear Discriminant Analysis (LDA)

The goal of the LDA is reducing the number of the features to one while maintaining the most information that can be used to separate classes. We seek to find a line with coefficients w to project the data samples on that results in the highest separation between classes. To better separate the two classes, we seek to maximize the objective function shown in Equation 1:

$$J(w) = |\hat{\mu}_1 - \hat{\mu}_2|^2 / (\tilde{s}_1^2 + \tilde{s}_2^2) \quad (1)$$

In this equation, $(\hat{\mu}_i)$ denotes the mean of i th class after projection, and \tilde{s}_i denotes the scatter within class i [10]. To find the optimum w , we first rewrite the objective function as shown in Equation 2:

$$J(w) = w^T S_B w / w^T S_W w \quad (2)$$

Where S_B and S_W are the between-class and within-class scatter matrices.

By derivation of Equation 2 with respect to w and equating it to zero, we reach the optimum value of w^* , which is obtained as follows (Equation 3) [11]:

$$w^* = S_W^{-1}(\hat{\mu}_1 - \hat{\mu}_2) \quad (3)$$

2.5.2. Linear Support Vector Machine (Linear SVM)

In the linear SVM, we look for the optimum hyperplane (w) that has the largest margins between the two groups. To find the optimum hyperplane, we minimize the objective function (Equation 4) considering the constraints (Equation 5) using Lagrange coefficients.

$$J(w) = \frac{1}{2} \|w\|^2 \quad (4)$$

$$y_i(w^T x_i + w_0) \geq 1 \quad (5)$$

In these equations, W is the plane separating the two classes, W_0 is the bias term, x_i s are the support vectors and y_i -s are their class labels ($C_1=+1$ and $C_2=-1$). The final answer to this optimization problem is equal to:

$$w^* = \sum_{i=1}^N \lambda_i x_i y_i \quad (6)$$

λ_i = Lagrange coefficients

The class of data sample x can be determined using the following formula:

$$w^{*T} x + w_0 \geq 1 \quad x \in C_1 \quad (7)$$

$$w^{*T} x + w_0 \leq -1 \quad x \in C_2 \quad (8)$$

2.5.3. Support Vector Machine with RBF Kernel

SVM with RBF kernel solves the classification problem in a higher dimensional space which allows the classifier to separate the two classes that are non-linearly separable. By using the RBF kernel, the data is transformed to a very high-dimensional space and afterward, the SVM is used to classify the data. An RBF kernel has the general form of Equation 9 [11]:

$$K(x_1, x_2) = \exp\left(-\frac{\|x_1 - x_2\|^2}{\sigma^2}\right) \quad (9)$$

In this formula, x_1, x_2 are two vectors and σ^2 is the variance parameter. Also, the optimization problem is as Equation 10:

$$\text{MAX}(\sum_i \lambda_i - \frac{1}{2} \sum_{ij} \lambda_i \lambda_j y_i y_j K(x_i, x_j)) \quad (10)$$

$$\text{Subject to: } 0 \leq \lambda_i \leq C, \quad I = 1, 2, \dots, N \ \& \ \sum_i \lambda_i y_i = 0$$

In this equation, C is a constant positive coefficient. By solving Equation 10 via Lagrange coefficients, we get Equation 11 for determining the class of data sample x when the classes are not linearly separable [12].

$$g(x) = \sum_{i=1}^{Ns} \lambda_i y_i K(x_i, x) + w_0 \quad (11)$$

$$\text{if } g(x) > (<) 0 \text{ class is } C_1(C_2)$$

2.5.4. K-Nearest Neighbors (KNN)

In the KNN classifier, the class of an unknown data sample is determined according to the density of points related to each group in the K neighbors closest to the unknown data sample [11]. The unknown data sample is assigned to the category that is most repetitive among its K nearest neighbors.

3. Results

In this section, we report the classification accuracy of each classifier, which has been fed with all the subsets of the above-mentioned features. Finally, the optimum classifier and the best features will be determined and discussed.

3.1. LDA

Initially, the features were used individually as inputs to the LDA classifier, and the results are shown in Table 2. The maximum classification accuracy in one-dimensional

space was obtained using both single-features F3 and F9, and is 96.14% but F9 leads to a smaller standard deviation.

Table 2. The classification accuracy obtained using every single feature as input of the LDA classifier

Feature	Testing Accuracy (%) (mean ± std)
F1	95.68 ± 13.79
F2	95.68 ± 13.78
F3	96.14 ± 13.55
F4	96.07 ± 13.47
F5	95.99 ± 13.44
F6	95.91 ± 13.44
F7	95.99 ± 13.42
F8	95.83 ± 13.44
F9	96.14 ± 13.4

3.2. Linear SVM

As shown in Table 3, using the linear SVM, in one-dimensional space the maximum average accuracy of %96.30 is obtained using F9.

Table 3. The classification accuracy obtained using every single feature as input of the linear SVM classifier

Feature	Testing Accuracy (%) (mean ± std)
F1	95.83 ± 13.56
F2	95.68 ± 13.67
F3	95.91 ± 13.59
F4	95.99 ± 13.52
F5	95.91 ± 13.51
F6	95.99 ± 13.48
F7	95.99 ± 13.45
F8	95.99 ± 13.44
F9	96.30 ± 13.37

3.3. RBF SVM

To determine the suitable standard deviation (σ) of the radial basis kernel, we determined the maximum accuracy obtained from different values of σ in one-dimensional space. The maximum accuracy was obtained for $\sigma=0.25$. The classification accuracy using every single feature and the SVM classifier with the RBF kernel with $\sigma=0.25$ is given in Table 4. As shown in Table 4, using the radial SVM, in one-dimensional space the maximum average accuracy of %96.37 is obtained using F8.

Table 4. The classification accuracy obtained using every single feature as input of the RBF SVM classifier with $\sigma=0.25$

Feature	Testing Accuracy (%) (mean ± std)
F1	96.14 ± 13.09
F2	91.75 ± 16.02
F3	95.53 ± 15.39
F4	63.44 ± 17.12
F5	84.58 ± 17.37
F6	94.21 ± 16.81
F7	92.6 ± 16.63
F8	96.37 ± 16.22
F9	88.43 ± 16.00

3.4. KNN

At first, the proper value of K was unknown to us, and we tested the KNN in the range of K between 1 and 13. In one-dimensional space, the maximum average accuracy of 96.68% was obtained using F8 and K=5 neighbors. As a result, we consider only K=5 nearest neighbors. The results of using all single features and KNN classifier with K=5 are shown in Table 5.

3.5. Optimum Features

After determining the best single features for each classifier, we want to determine the best subset of features that lead to the highest classification accuracy. For this purpose, we report the maximum classification accuracy obtained by each classifier in Table 6 and the corresponding best features are illustrated in Table 7. Because the

Table 5. The classification accuracy obtained using every single feature as input of the KNN classifier with K=5

Feature	Testing Accuracy (%) (mean ± std)
F1	66.44 ± 14.95
F2	93.52 ± 15.75
F3	95.68 ± 15.14
F4	77.4 ± 16.55
F5	84.27 ± 17.36
F6	63.81 ± 16.84
F7	93.14 ± 16.57
F8	96.68 ± 16.13
F9	88.5 ± 15.9

Table 6. Maximum classification accuracy obtained by different classifiers

Classifier	Testing Accuracy (%) (mean \pm std)	Confusion Matrix	Optimum Feature Set
KNN	96.68 \pm 16.13	$\begin{matrix} 1 & 0 \\ 0.066 & 0.933 \end{matrix}$	F8
LDA	96.22 \pm 13.58	$\begin{matrix} 1 & 0 \\ 0.075 & 0.924 \end{matrix}$	F4, F6
SVM (Linear)	96.76 \pm 12.77	$\begin{matrix} 1 & 0 \\ 0.064 & 0.935 \end{matrix}$	F3, F4, F5, F9
SVM (RBF)	96.91 \pm 13.03	$\begin{matrix} 1 & 0 \\ 0.061 & 0.938 \end{matrix}$	F3, F4, F5, F7

maximum average accuracy among all classifiers is 96.91%, which was obtained using the RBF SVM, in our opinion the features that led to this accuracy (F3, F4, F5, and F7) may be considered as the best feature subset. Consequently, Peak amplitude asymmetry, peak to trough ratio, recovery slope, and duration between peaks are the selected features.

Now we want to prioritize these four features. For this purpose, we inspect the average classification accuracy obtained using each of these four features and RBF SVM classifier as shown before in Table 4. Since F3 results in the highest accuracy, it can be considered as the most effective feature, followed by F7, F5, and F4.

Table 7. Features that led to the highest classification accuracy using each classifier

Feature	Classifier			
	KNN	LDA	SVM (Linear)	SVM (RBF)
F1				
F2				
F3			*	*
F4		*	*	*
F5			*	*
F6		*		
F7				*
F8	*			
F9			*	

4. Discussion

We aim to compare the optimum classification accuracy we obtained by the RBF SVM classifier (because it resulted in the highest accuracy) with the accuracy resulted using RBF SVM and the same classification

approach as we used but using the features proposed in other articles although for clustering the neurons and not classifying them. As can be seen in Table 8, the highest average classification accuracy using the features mentioned in the past articles is 96.24% which is obtained using features F1 and F3. However, the highest average classification accuracy we obtained (96.91%) shows an improvement of 0.67%. In the absence of validation methods such as optogenetics, some articles use electrophysiological methods such as inhibitory and excitatory groups. Although classification was done on neurons of mouse hippocampus, our proposed scheme may be applicable to other species like humans and monkeys and other brain regions as well, which would be a proper option to expand this research.

5. Conclusion

In this paper, we classified the mouse hippocampus neurons into inhibitory and excitatory categories using eight shape features of spike waveforms in addition to their firing rates, and applying LDA, KNN, and SVM classifiers. We showed RBF SVM was the best classifier for functional separation of mouse brain's neurons. Also, we showed Spike asymmetry, Peak-to-trough ratio, Recovery slope, and Duration between peaks were the most discriminative features to classify neurons into

spike train cross-correlation to validate their clustering results. Validation with optogenetics is provided when the species under test is of the parvalbumin category and also optogenetic stimulation tools are present at the same time.

It is noteworthy that, different features of firing rates were used in [13] to discriminate inhibitory and excitatory neurons using a clustering scheme. However, no classification scheme was proposed in that paper to assess the classification accuracy using those proposed

Table 8. Classification accuracy of RBF SVM using different features proposed in the past articles

Reference	Features	Testing Accuracy (%) (mean \pm std)	Confusion matrix	
[14], [15]	F9	90.32 \pm 13.31	0.8656 0.0592	0.1344 0.9408
[8], [7]	F1	95.68 \pm 7.33	1 0.0864	0 0.9136
[16]	F2, F9	91.76 \pm 8.71	0.9872 0.152	0.0128 0.848
[17]	F1, F3	96.24 \pm 6.55	0.9984 0.0736	0.0016 0.9264
[18]	F1, F4, F5, F6	95.04 \pm 7.58	0.9664 0.0656	0.0336 0.9344
Our method	F3, F4, F5, F7	96.91 \pm 13.03	1 0.061	0 0.938

features. Applying our proposed classification approach using RBF SVM on the firing rate features proposed in [13] to compare the classification performance of that feature set would be future work. Although, as shown in Table 8, firing rate alone (F9) or in combination with shape features F1:F8 are not optimum for the classification of inhibitory and excitatory neurons since the shape features of spike waveforms resulted in the optimum classification accuracy.

Acknowledgments

We would like to offer our special thanks to professor Buzsaki for making his datasets freely available, and also to Iran Cognitive Sciences and Technologies Council for its support.

References

- 1- C. O. Donnell, J. T. Gonc, and C. Portera-cailliau, "Beyond excitation / inhibition imbalance in multidimensional models of neural circuit changes in brain disorders," [Online]. Available: <https://www.ncbi.nlm.nih.gov/pmc/articles/PMC5663477/>, 2017.
- 2- Petilla Interneuron Nomenclature Group (PING), "Petilla terminology: nomenclature of features of GABAergic interneurons of the cerebral cortex," *Nature reviews. Neuroscience*, vol. 9, no. 7, pp. 557–568, 2008.
- 3- D. F. English, S. Mckenzie, T. Evans, K. Kim, E. Yoon, and G. Buzsáki, "Pyramidal cell-interneuron circuit architecture and dynamics in hippocampal networks," *Neuron*, vol. 96, no. 2, pp. 505–520, 2018.
- 4- M. Pachitariu, Marius, Nicholas Steinmetz, Shabnam Kadir, and Matteo Carandini, N. Steinmetz, S. Kadir, M. Carandini, and K. D. Harris, "Kilosort: realtime spike-sorting for extracellular electrophysiology with hundreds of channels," *BioRxiv*, p. 061481, 2016.
- 5- Nowak, Lionel G., Rony Azouz, Maria V. Sanchez-Vives, Charles M. Gray, and David A. McCormick, "Electrophysiological Classes of Cat Primary Visual Cortical Neurons In Vivo as Revealed by Quantitative Analyses," *ournal of neurophysiology*, vol. 89, no. 3, pp. 1541–1566, 2003.
- 6- M. Avermann, C. Tomm, C. Mateo, W. Gerstner, and C. C. H. Petersen, "Microcircuits of excitatory and inhibitory neurons in layer 2 / 3 of mouse barrel cortex," *J. Neurophysiology*, vol. 107, pp. 3116–3134, 2012.
- 7- A. Sirota, S. Montgomery, S. Fujisawa, Y. Isomura, and G. Buzsáki, "Entrainment of neocortical neurons and gamma oscillations by the hippocampal theta rhythm," *Neuron*, vol. 60, no. 4, pp. 683–697, 2009.
- 8- Jia, Xiaoxuan, Joshua H. Siegle, Corbett Bennett, Samuel D. Gale, Daniel J. Denman, Christof Koch, and Shawn R. Olse, "High-density extracellular probes reveal dendritic backpropagation and facilitate neuron classification," *journal of neurophysiology*, vol. 121, no. 5, pp. 1831–1847, 2019.
- 9- H. Cheng, D. J. Garrick, and R. L. Fernando, "Efficient strategies for leave-one-out cross validation for genomic best linear unbiased prediction," *Anim. Sci. Biotechnol.*, vol. 8, no. 38, pp. 1–5, 2017.
- 10- K. Fukunaga, in *Introduction to statistical pattern recognition*, San Diego: Academic Press Professional, pp. 132–153.

- 11- R. Duda and P. Hart, "Pattern Classification," *New York: Wiley-Interscience*, 2000, pp. 174–188.
- 12- S. Theodoridis and K. Koutroumbas, in *Pattern Recognition*, California: *Academic Press*, 2009.
- 13- Becchetti, Andrea, Francesca Gullo, Giuseppe Bruno, Elena Dossi, Marzia Lecchi, and Enzo Wanke, "Exact distinction of excitatory and inhibitory neurons in neural networks: a study with GFP-GAD67 neurons optically and electrophysiologically recognized on multielectrode arrays," *Frontiers in neural circuits*, vol. 6, p. 63, 2012.
- 14- D. A. McCormick, B. W. Connors, J. W. Lighthall, and D. A. Prince, "Comparative Electrophysiology of Pyramidal and Sparsely Spiny Stellate Neurons of the Neocortex," *J. neurophysiology*, vol. 54, no. 4, October 1985.
- 15- J. A. Cardin, L. A. Palmer, and D. Contreras, "Stimulus Feature Selectivity in Excitatory and Inhibitory Neurons in Primary Visual Cortex," *J. Neurosci*, vol. 27, no. 39, pp. 10333–10344, 2007.
- 16- Henze, Darrell A., Zsolt Borhegyi, Jozsef Csicsvari, Akira Mamiya, Kenneth D. Harris, and Gyorgy Buzsaki, "Intracellular Features Predicted by Extracellular Recordings in the Hippocampus In Vivo," *Journal of neurophysiology*, vol. 84, no. 1, pp. 390-400, 2000.
- 17- S. Y. Shin and M. A. Sommer, "Activity of Neurons in Monkey Globus Pallidus During Oculomotor Behavior Compared With That in Substantia Nigra Pars Reticulata," *Neurophysiology*, vol. 103, no. 4, pp. 1874–1887, 2010.
- 18- J. F. Mitchell, K. A. Sundberg, and J. H. Reynolds, "Differential Attention-Dependent Response Modulation across Cell Classes in Macaque Visual Area V4," *Neuron*, vol. 55, no. 1, pp. 131–141, 2007.